

# Particle Environment Surrounding the Midcourse Space Experiment Spacecraft

Gary E. Galica,\* B. David Green,<sup>†</sup> and Mark T. Boies<sup>‡</sup>  
*Physical Sciences, Inc., Andover, Massachusetts 01810*  
O. Manuel Uy,<sup>§</sup> David M. Silver,<sup>¶</sup> Richard C. Benson,\*\* and Robert E. Erlandson<sup>††</sup>  
*Johns Hopkins University, Applied Physics Laboratory, Laurel, Maryland 20723*  
Bob E. Wood<sup>‡‡</sup>  
*Sverdrup Technology, Inc., Arnold Air Force Base, Tennessee 37389*  
and  
David F. Hall<sup>§§</sup>  
*The Aerospace Corporation, El Segundo, California 90245*

Particle occurrence rates, velocities, size distributions, and trends in the environment have been measured above the Midcourse Space Experiment spacecraft using optical sensors. Results from the spacecraft's first 11 months on orbit are presented. Particles were detected both in association with known particle-generating activities and during comparatively quiescent times. In general, the optical environment is quite benign. The on-orbit environment appears to be dominated by particles remaining from ground processing operations. That environment is consistent with prelaunch cleanliness level measurements. Particulates were detected during quiescent periods as the spacecraft passed through the terminator from eclipse into daylight. Particle evolution occurs within minutes of solar heating onset. At Midcourse Space Experiment altitudes, drag effects are not significant until comparatively long times ( $10^3$ – $10^4$  s); therefore, the observed velocities of the near-field particles, in the 1–10-cm/s range, are representative of the surface release velocity. The particles are observed in the 1–100- $\mu$ m-size range. The size distribution scales approximately as  $r^{-1.5}$  down to the sensitivity limit.

## Introduction

NEAR-FIELD contamination from particulates released from a spacecraft poses a significant threat to the performance of optical sensors. Particles have been observed on most space missions including Mercury, Apollo, Skylab, Shuttle,<sup>1</sup> and Magellan spacecraft. Particulates reduce sensor performance both by depositing on sensitive optical surfaces and also by generating spurious signals when in a sensor's field of view. Particulates manifest themselves in imaging systems by scattering sunlight and earthshine and by their thermal radiation.<sup>2,3</sup> These signals can take the form of spurious discrete signals as well as an overall increase in the background signal due to out-of-focus image features.

Particulates released on orbit have several sources. Dust particles and ice crystals carried up from the ground at launch will be released from the spacecraft.<sup>1</sup> Past investigations have shown that this initial contamination decays with time, and after a few days to weeks the particulate environment decays to a more benign level.<sup>4,5</sup> In addition, thermal expansion and contraction, such as that experienced during terminator crossings, will continue to generate and

release additional particulate matter during a mission.<sup>6</sup> Mechanical operations such as door openings, solar panel deployments, and spacecraft maneuvering have the potential to release large numbers of particulates. Perhaps the most insidious, and most poorly quantified, source of particulates is the degradation of materials. After exposure to the space environment, including atomic oxygen, solar radiation, energetic particles, and orbital debris, many materials degrade and subsequently begin to release particulate and gaseous matter. The rate at which this occurs on an operational spacecraft for a long-duration mission is unknown.

In the absence of charging or strong mechanical shocks, we expect the particles to leave the surface with only a small velocity relative to the spacecraft. The molecules of the tenuous upper atmosphere collide with the particles at 8-km/s velocity and exert drag, forcing the particles to slow relative to the atmosphere (but accelerate away from the spacecraft). Velocities and accelerations relative to the spacecraft  $x$ ,  $y$ ,  $z$  coordinate system allow a particle to move through the optical sensors' fields of view after it leaves the spacecraft surfaces. The particle's trajectory during the optical system integration time gives rise to a particle track in the detected image. The trajectories expected for particles at the Midcourse Space Experiment (MSX) mission altitude of 903 km have been calculated previously.<sup>7</sup> Particles will be in the optical field of view either by having a trajectory pass directly through the near-field observed volume, or a trajectory initially to the windward of the optical axis that is swept by drag back into the observation volume. Particles are expected to remain in the vicinity of the spacecraft and be accelerated over a 100–10,000-s period.

Particles generated from spacecraft surfaces will interfere with the remote sensing of emissions from objects in space, the Earth, and its upper atmosphere. We have previously reviewed the sources, sizes, and composition of particles observed in local spacecraft environments, presented predictions of the optical signatures these particles would generate and presented predictions of the signatures of these near-field particles as detected by spacecraft optical systems.<sup>3</sup> Particles can be remotely detected across the ultraviolet–infrared (UV–IR) spectral region by their thermal emission, scattered sunlight, and earthshine. The spectral-bandpass-integrated signatures of

Received 2 June 1998; revision received 24 November 1998; accepted for publication 27 November 1998. Copyright © 1999 by the American Institute of Aeronautics and Astronautics, Inc. All rights reserved.

\*Principal Research Scientist, Research Division, 20 New England Business Center.

<sup>†</sup>Executive Vice President, Research Division, 20 New England Business Center. Senior Member AIAA.

<sup>‡</sup>Principal Research Scientist, Research Division, 20 New England Business Center. Member AIAA.

<sup>§</sup>Principal Professional Chemist, Technical Services Department, Johns Hopkins Road. Member AIAA.

<sup>¶</sup>Principal Staff Senior Scientist, Applied Research and Technology Department, Johns Hopkins Road.

\*\*Principal Professional Chemist, Applied Research and Technology Department, Johns Hopkins Road. Member AIAA.

<sup>††</sup>Senior Staff Physicist, Space Department, Johns Hopkins Road. Member AIAA.

<sup>‡‡</sup>Senior Engineer, Applied Technology/Optical Diagnostics Group, Arnold Engineering Development Center. Associate Fellow AIAA.

<sup>§§</sup>Senior Scientist, Surface Sciences Department, 2350 E. El Segundo Boulevard. Senior Member AIAA.

these particles (dependent on size and composition) are then mapped back onto the UV, visible (VIS), and IR sensor systems. At distances less than kilometers, these particles are out of focus for telescoped imaging systems. The image produced is blurred over several pixels.

Solar illumination determines the observed signature and detection limits in the UV and VIS, whereas self-emission and scattered earthshine radiances will produce the IR signature.<sup>2,3</sup> Visible light film camera-based observations of the environment surrounding the Shuttle have provided an extensive particle observational data set.<sup>4,8</sup> Size distributions peak to smaller radius particles. Particle velocities relative to the spacecraft on the order of meter per second were observed.<sup>8</sup> Activities, such as maneuvers, mechanical operations, and even terminator crossings, induced the release of particles from surfaces. IR emission from particles was observed by the cryogenic IR radiance instrumentation for Shuttle radiometers and interferometer during Shuttle mission STS39 (Ref. 3). Particles over the centimeter to 100- $\mu\text{m}$  range were detected in the field of view for several seconds.

Short-duration missions will be dominated by the release of particles brought to orbit from the ground and ascent environments. On extended-duration missions, after these ground-origin particles have evolved from surfaces, additional particles will be created by erosion, abrasion, impacts, and thermal stresses. A long-duration orbital database on the magnitudes of these processes does not exist. The MSX is the first mission to provide quantitative information from onboard environmental monitors that permits an assessment of the thorough contamination control plan that guided its design, assembly, and handling.<sup>9</sup> Previous space missions have lacked either a detailed plan, sufficient instruments for verification, or were of too short duration to provide guidance for designers of future spacecraft. Because particles can arise from both ground and orbital sources, both a contamination control plan and monitoring instruments are required.

The MSX spacecraft comprises a suite of fully characterized, carefully calibrated, very sensitive optical instruments with broad spectral imaging capability. Its primary mission is to precisely measure the optical signatures from a broad range of natural phenomena, as well as man-made targets. Optical measurements spanning from the far UV (110 nm) to the very long wavelength IR (28  $\mu\text{m}$ ) spectral region are performed in a series of systematic measurement sequences or data collection events (DCEs). The mission objectives and instrumentation have been described previously.<sup>10,11</sup> This sophisticated spacecraft is  $1.5 \times 1.5 \times 5.1 \text{ m}^3$ , has mass of  $\sim 2700 \text{ kg}$ , and has a designed mission lifetime of 4 years. The MSX spacecraft was launched from Vandenberg Air Force Base into a circular 99-deg near sun-synchronous 904-km-altitude orbit by a Delta II booster on April 24, 1996.

Most of the external surfaces of MSX are covered with multilayer insulation (MLI) comprising 20 layers of aluminized mylar separated by Dacron<sup>®</sup> netting with the innermost surface and exterior layers being silver/indium tin oxide coated Teflon<sup>®</sup> or beta cloth.<sup>12</sup> Attitude maneuvering is achieved via reaction wheels to eliminate thrust exhaust contamination effects. To help ensure the desired operational performance, a thorough contamination control plan for material selection and handling was implemented. Furthermore, a suite of contamination instruments was included in the manifest to monitor performance during the ground processing and integration and on orbit. We present results of the particulate environment measurements from the first 11 months on orbit. This time period comprises the cryogen phase of the MSX mission.

The primary optical sensors and contamination instruments were assembled, tested, and integrated under carefully controlled conditions.<sup>9</sup> Contamination control was an integral part of the MSX program. Design, materials selection, multiple instrumented bake-outs, ground assembly, handling, and bagging addressed contamination concerns. Visual and tape lift inspections were performed frequently. Cleaning (vacuum and alcohol wipe) was performed as required. In spite of the multiple year assembly process, the spacecraft external surfaces were measured to be about level 318 for particles with no measurable molecular films at 1 month before launch. The MSX external contamination model<sup>17,12</sup> predicts molecular, particulate, and electromagnetic effects with the source terms based on the MSX contamination control plan and laboratory and flight mea-

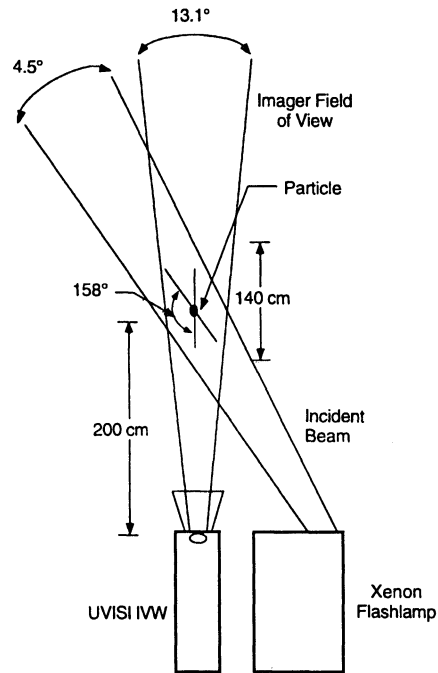


Fig. 1 XF/UVISI IVW particle detection configuration.

surements. Transport, deposition, and the effects produced are also modeled. This model provides detailed predictions and creates the essential linking of each contamination sensor's observations.

### Data Collection

The xenon flashlamp (XF) is one of a suite of instruments that monitor the particulate and gaseous contamination environments of MSX. The near-field particulate is illuminated by high-intensity visible radiation from the XF (or by the sun) in the field of view of the ultraviolet and visible imagers and spectrographic imagers (UVISI), wide-field-of-view visible imager (IVW). The flashlamp particle experiment has been described in detail previously.<sup>13</sup> Radiation scattered by illuminated contaminant particles within its  $10.5 \times 13.1$  deg field of view is imaged by the IVW. The intensity of the scattered radiation is related to a particle's size and composition. The particle's track yields information about its velocity and trajectory. From ground calibration data, we estimate a sensitivity sufficient to detect particles smaller than  $1 \mu\text{m}$  and to determine cross-field velocities from  $1 \text{ mm/s}$  to  $50 \text{ m/s}$ . The UVISI IVW is the primary sensor used to characterize the near-field particulate environment. The IVW and other MSX imagers are used to characterize the far-field particulate environment<sup>14</sup> (Fig. 1).

The first particle measurements occurred approximately 34 h after launch. Particle observations were made periodically during the cryophase of the mission (the first 11 months on orbit). Most of these DCEs comprise 3–12 min of actual observation time. During this phase of the mission, approximately three DCEs per week were performed. The DCEs are distributed with respect to latitude. Specialized DCEs are designed to make observations during terminator crossings and discrete events, such as cover openings and rapid maneuvers. This presentation focuses on the long-term trends in the environment. The data from the cover deployments are discussed briefly, but are not included in the long-term trend data.

### Particle Environment

#### Particle Occurrence Rates

To provide one indicator of the overall particulate environment, we determined the fraction of image frames during a particular measurement or measurements that contained detectable particle signatures. Only DCEs with appropriate illumination conditions and imager settings are considered. This measure is based on the visible imagery obtained from the UVISI IVW with either solar or flashlamp illumination.

The graph shown in Fig. 2 represents a monthly average of this particle occurrence rate from the second day of the mission through

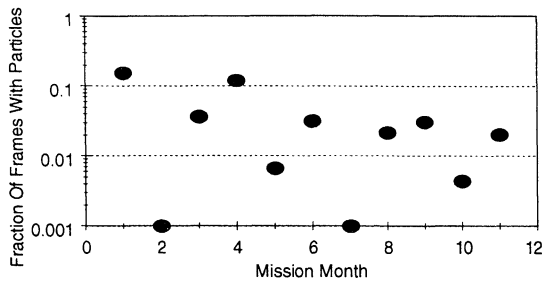


Fig. 2 Fraction of image frames contaminated with particle signatures as a monthly average.

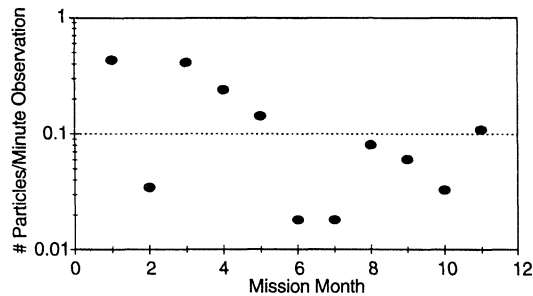


Fig. 3 Number of particles observed per minute of observation time as a monthly average.

the cryophase [12 four-week mission months (MM)]. Figure 2 represents this environment in terms of the effect on optical sensors, i.e., the fraction of image frames containing particulates. From DCE to DCE, the particle occurrence rate varies greatly with anywhere from half the images containing particles to essentially no frames containing particles ( $<0.001$ ). The monthly average particle occurrence rate is, of course, less variable and has at most 15% of images containing particles. Each DCE comprises 3–12 min of observation time. Each image frame is 0.5 s in duration.

Figure 3 shows the trend in the particulate environment in terms of the actual number of particles observed per minute of observation time averaged over the month. We obtained 20–40 min of observation time each MM.

The particulate occurrence rate has decreased steadily since the start of the mission (Fig. 3). During the first month of the mission, we observed  $\sim 0.4$  particles per minute of observation time, whereas at the end of the cryophase (MM 12) that rate was nearly 10-fold less. Even by averaging of the DCEs in an MM, the particulate environment appears highly variable and probably reflects the various activities and DCEs of this complex spacecraft. Although there is large variability, there is a downward trend. This decay corresponds approximately to time $^{-0.8}$ .

#### Velocity Distribution

Even at the start of the mission, more than one-half of the individual DCEs were free of particulate contamination. In the monthly average, 15% of the image frames contained particles. When particles were present, however, a sizeable fraction of frames were contaminated. This phenomenon is due to the slow particle velocities. In contrast to the particulates observed surrounding the Shuttle, the particulates released from MSX travel at slow velocities. At Shuttle altitudes, particles are quickly accelerated by drag and are swept quickly through the field of view of a sensor. Average particle velocities measured from the Shuttle are in the 1-m/s range.<sup>8</sup> At MSX altitudes, however, the effect of drag is small except for the very smallest particles ( $<1 \mu\text{m}$ ). Particles apparently are released from the spacecraft with relatively slow velocities and, hence, stay in the field of view of an optical sensor for a long period of time. As a result, a small number of particles can contaminate a proportionately larger number of image frames. The observed velocity distribution, therefore, is an accurate measure of the release velocities.

Figure 4 shows the velocity distribution of  $\sim 50$  particles released from the MSX spacecraft during the first 11 months on orbit. We have described the particle velocity determination previously.<sup>13</sup> Briefly, a particle's range and downrange velocity are determined

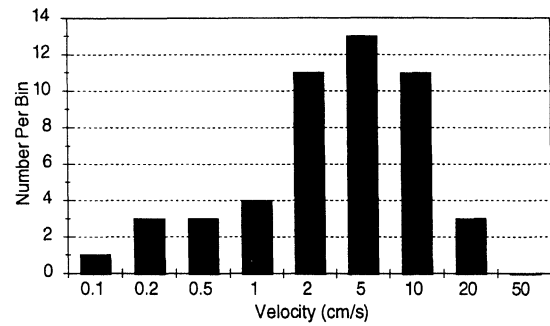


Fig. 4 Particle velocity distribution.

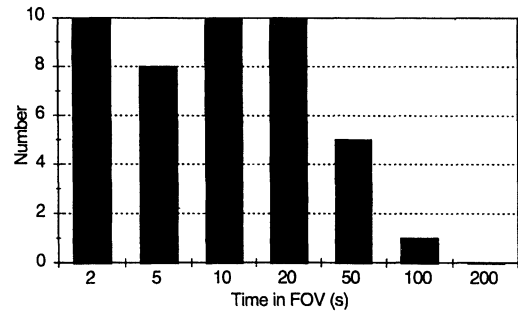


Fig. 5 Particle residence times in UVISI IVW field of view ( $10.1 \times 13.6$  deg).

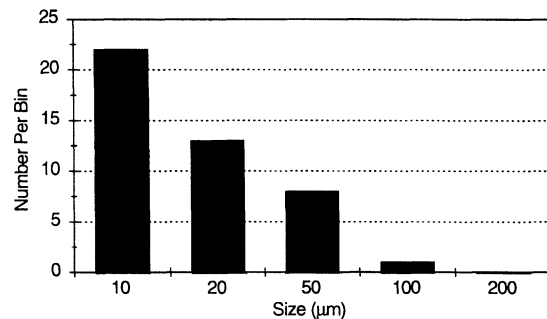


Fig. 6 Particle size distribution.

from the blur circle and its temporal behavior. The cross-field velocities are determined by tracking particles in successive image frames. Uncertainties in the range are typically 25%. Uncertainties in the velocity are typically 40%. Release velocities are slow, peaking in the 5–10 cm/s range. The average distribution of residence times for particles in the UVISI IVW is shown in Fig. 5. The UVISI IVW has a  $10.5 \times 13.1$  deg field of view. Because the particles represented in this distribution were observed in the near field of the spacecraft (distances  $<4$  m), the residence times are long, but finite. Particles in the far field, with comparable cross-field velocities, will have proportionately longer residence times. It is conceivable that a single particle could remain in the field of view of a sensor for an entire DCE.

#### Size Distribution

Figure 6 shows the size distribution for the quiescently released particles. We have described the estimate of particle size previously.<sup>13</sup> The UVISI IVW sensor and the XF have been radiometrically and spatially calibrated very accurately. The solar irradiance is also known very accurately. The particle scattering cross section is determined directly from the calibrated imagery and the illumination conditions. The cross section can be determined with an uncertainty of about 50%.

To estimate particle sizes, however, we must assume an albedo for the particle. For these data, we have assumed an albedo of 0.1. The visible wavelength albedos of typical spacecraft materials range from approximately 0.04–0.4 (Ref. 3). Carbon, common in black paint, has an albedo of  $\sim 0.04$ ; silver and aluminum, common in MLI, have albedos of  $\sim 0.4$ . The derived particle size depends only

on the square root of the albedo; therefore, a factor of three uncertainty in particle size due to the uncertainty in the assumed albedo is reasonable. The size distribution (for  $r > 10 \mu\text{m}$ ) peaks at the small particle sizes. For particles larger than  $10 \mu\text{m}$ , the distribution closely follows an  $r^{-1.2}$  dependence.

The minimum detectable particle size depends on the gain state and configuration of the UVISI IVW imager. The gain state is determined primarily by the observational background. For example, for a nighttime celestial view, the gain will be set close to its maximum. In that case, the minimum detectable particle size is less than  $1 \mu\text{m}$ . For daytime DCEs, with sun angles close to the sensor line of sight, solar glint may limit the gain of the sensor. In that case, particles smaller than  $10 \mu\text{m}$  are undetectable. Even at these lower gain states,  $10\text{-}\mu\text{m}$  particles were easily detectable. As a result, particles larger than  $10 \mu\text{m}$  are detectable almost irrespective of imager settings. However, particles smaller than  $10 \mu\text{m}$  are only detectable with optimized imager settings.

When we assemble a distribution, therefore, all DCEs are available for particles larger than  $10 \mu\text{m}$ , whereas only a small subset of DCEs are appropriate for particles smaller than  $10 \mu\text{m}$ . Many smaller particles were detected during the mission; however, they are not incorporated into the present distribution.

The velocity distributions for small ( $r < 12 \mu\text{m}$ ) and large ( $r > 30 \mu\text{m}$ ) particles are shown in Fig. 7. The large particle velocity distribution is shifted somewhat toward higher velocity. There is not a dramatic difference in the distributions, however, except for a lack of low-velocity large particles. This slight difference in the distributions may indicate a somewhat different mechanism for release of large particles than for small particles.

#### Environment Trends

The size distribution is shown as a function of time in Fig. 8. The distribution for the first MM is compared to that for the remainder of the cryogen phase. There is a definite shift to larger particles after the first MM. The size distribution from MM 1 follows an  $r^{-1.6}$  size distribution. This size dependence is in agreement with previous size distribution measurements from short-duration missions.<sup>1,4,6,8</sup> The small particles from the MM 2 to MM 12 distribution also follow a similar distribution ( $r^{-1.7}$ ); however, a distinct contribution from larger particles is present. This result is consistent with the scaling of adhesive force with particle size.

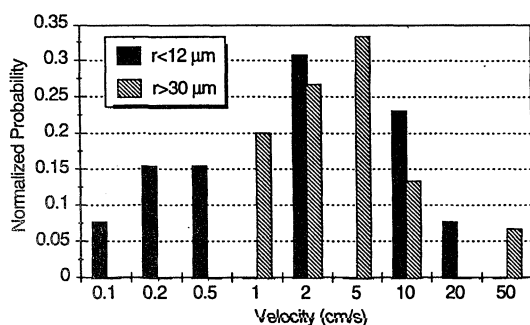


Fig. 7 Particle velocity distributions for small particles ( $r < 12 \mu\text{m}$ ) and large particles ( $r > 30 \mu\text{m}$ ).

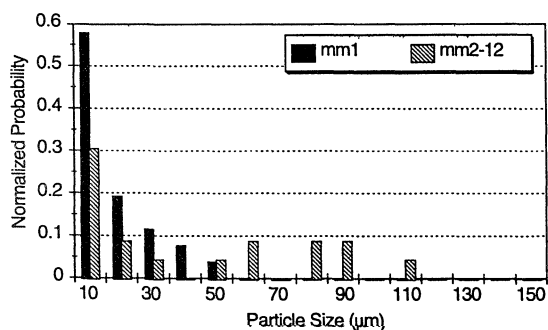


Fig. 8 Comparison of particle size distribution from MM 1 and MM 2-12 on orbit.

The adhesive force for a sphere on a flat plane in vacuum is given by

$$F = 4\pi\gamma_s r$$

where  $\gamma_s$  is the surface energy of the sphere material and  $r$  is the sphere radius.<sup>15</sup> Although the particles observed are not likely spheres and the spacecraft surfaces are not planes, the overall dependency of the force on particle size should remain approximately valid. The adhesive force is larger for larger particles and smaller for smaller particles. For an equilibrium process, e.g., thermal or solar illumination, one would expect that the smaller particles are more easily (more quickly) removed from spacecraft surfaces than larger particles. For the case of a shock, such as that due to a cover opening or micrometeoroid impact, the opposite will be true. Because the force felt by a particle during an acceleration increases as the mass of the particle (or  $r^3$ ), the larger particles are more likely to be released than the smaller particles. We have purposely excluded the cover opening data from the present analysis; therefore, we expect to observe a size distribution characteristic of equilibrium processes (more small particles than large). Our results are consistent with this model.

#### Release Mechanisms

Measurements previously taken on the Shuttle have shown a strong dependency between umbra exit and particle release.<sup>6</sup> Similar results are observed on MSX. After a delay of approximately 2 min, particles begin to appear in the sensor field of view. The particle release continues for the several minute duration of the experiment. These umbra exit particulate releases have continued throughout the mission with the number of particles released decaying as basically the same rate as the overall trend.

In addition to the umbra exits, slewing of the spacecraft also releases particles. At the conclusion of a DCE with a fixed attitude (for example, a particular ram angle or sun angle), the spacecraft slews back to its nominal parked attitude. Often during these slews, particles are released. The spacecraft angular velocity is approximately  $1 \text{ deg/s}$ , whereas the particle observed angular velocity is approximately  $1.4 \text{ deg/s}$ . The linear velocity of the particle is very close to the linear velocity of the outer spacecraft surfaces at an angular velocity of  $1 \text{ deg/s}$ . This seems to indicate that during slewing particulates are released with low relative velocities.

#### Comparison with Cleanliness Levels

Results of tape lifts taken from various spacecraft surfaces indicate that MSX surfaces were approximately at level 318 one month before launch.<sup>9</sup> A very small sample of tape lifts was taken several days before launch. These data indicated that the cleanliness levels were maintained despite a great deal of activity around the spacecraft in the days preceding launch. The spacecraft was generally double bagged and purged at all times. However, MSX was exposed with no bagging material for approximately 36 h while the fairing was installed around the spacecraft. Despite this activity, the contamination control measures taken during these operations were successful. The inside surfaces of the fairing were also cleaned to about level 300 as well. Even though particle redistribution will occur on ascent, the overall cleanliness level of the spacecraft was not expected to change.

By using the tape lift data, and the particle size distribution measured on orbit, we can estimate the number of particles on the spacecraft. The tape lift data indicate a percent area coverage (PAC) of 0.04%. A PAC of 0.04% corresponds roughly to a level 318 surface. From these data, we estimate that the number of observable particles ( $> 10 \mu\text{m}$ ) on the spacecraft at launch was approximately  $8 \times 10^5 \text{ m}^{-2}$ . We then can compare this estimated number of particles on the surface to the number actually observed to determine whether the particle environment is still dominated by particles brought up from the ground or by those created on orbit.

The average fraction of frames of the UVISI IVW that contain particles is 3%. These observations represent a total of 55 particles detected during 4.7 h of observation time. We will make the assumption that the particle release is more or less uniform in time and in its spatial distribution. Therefore, we can scale the observation rate by duty cycle and steradiancy factors to estimate the number of particles released from the spacecraft during the first year of the mission. The

duty cycle for particle observation is approximately  $5.8 \times 10^{-4}$ . The UVISIVW has a field of view of  $10.1 \times 13.6$  deg. If we then include the area of the entire spacecraft plus the solar panels, we estimate that  $7 \times 10^5$  particles/m<sup>2</sup> have been released from the spacecraft.

In addition to the steady-state, quiescent particle release rate, there were a few discrete events that released large numbers of particles. Within the first week of the mission, four impulsive cover openings were performed. The nine UVISI sensors deployed their covers in three separate groups, each group releasing an estimated 10,000–20,000 particles. The spatial IR imaging telescope cryogenic sensor also deployed its cover, releasing perhaps 20,000–40,000 particles. All told, these impulsive events released perhaps 50,000–100,000 particles. Although this is a large number of particles, it is a small contribution to the mission-integrated values.

The estimate of  $7 \times 10^5$  particles/m<sup>2</sup> based on observation is comparable to the  $8 \times 10^5$  particles/m<sup>2</sup> estimated from tape lift data taken before launch. The comparison of these estimates and the exponentially decreasing particle occurrence rate indicates that the MSX particulate environment has been dominated by surface contamination from ground operations. Particles produced by erosion on orbit have not contributed significantly to the environment during the first year on orbit. Other facets of the orbital environment surrounding MSX have been summarized elsewhere.<sup>16</sup>

### Conclusions

The MSX spacecraft has provided a unique opportunity to study particulate contamination, its sources, its trends, and its long-term effects. We have reached important conclusions about the particulate environment based on the first 11 months of mission data. We have detected particles both in association with known particle-generating activities and during comparatively quiescent times. Particles driven off during this period are likely those remaining from ground processing operations.

The particle occurrence rate follows at  $t^{-1}$  dependence, decaying from the first week on orbit to the present time, albeit with large variability. The particle size distribution ( $r > 10 \mu\text{m}$ ) approximately follows an  $\sim r^{-1.5}$  dependence with particles in the 1–200  $\mu\text{m}$  size range observed. The observed size distribution is in agreement with previous on-orbit measurements. The size distribution shows a shift toward larger particles as the mission progresses. This result agrees qualitatively with the simple description of the surface adhesion force. The adhesion force is directly proportional to the particle radius. Smaller particles should be released more easily, whereas larger particles should be released less easily.

Our estimate of the total number of particles released during the first 11 months is consistent with the measured surface cleanliness levels of MSX just prior to launch. From the observations, we conclude that the environment is dominated by particles remaining on surfaces from ground processing operations. There is no evidence that degradation of materials has occurred to a large extent on orbit. These results are probably due in large part to the comprehensive MSX contamination control plan, careful selection of spacecraft materials, and careful ground processing.

Particulates were detected during quiescent periods as the spacecraft passed through the terminator from eclipse into daylight. Particle evolution occurs within minutes of solar heating onset. This mechanism for particulate release has been documented previously. At MSX altitudes, drag does not significantly accelerate particles on these timescales and the observed velocities, in the 1–10 cm/s range, reflect those at surface release. There is very little dependence of the velocity distribution on particle size.

MSX, in its second year of operation, is continuing to acquire data on the particle environment. We hope to quantify whether the spacecraft reaches an asymptotic level of particle production, or whether particle production increases after multiple years on orbit as materials, structures, and mechanical systems age in the hostile space environment.

### Acknowledgments

This work was supported by the Ballistic Missile Defense Organization (BMDO), under the Midcourse Space Experiment (MSX)

Program Office, with Bruce Guilmain and Peter Kurucz as the MSX Program Managers at BMDO. The authors thank the members of the MSX Contamination Experiment Principal Investigator Team and the MSX Ultraviolet Visible Imagers and Spectrographic Imagers Instrument Team for their input and assistance. The authors gratefully acknowledge many useful discussions and great assistance from Alan Gelb and the MSX Operations team. These data have been peer reviewed by the MSX Principal Investigator Executive Committee and are approved for distribution outside the MSX community, in accordance with the MSX Data Release Policy (Revision 4, dated June 1997).

### References

- Green, B. D., "The Particle Environment On-Orbit: Observations, Calculations, and Implications," *Advances in Space Research*, Vol. 7, No. 5, 1987, p. 161.
- Rawlins, W. T., and Green, B. D., "Spectral Signatures of Micron-Sized Particles in the Shuttle Optical Environment," *Applied Optics*, Vol. 26, No. 15, 1987, pp. 3052–3060.
- Green, B. D., Mulhall, P. A., Rawlins, W. T., and Uy, O. M., "Optical Signatures of Particles in Space," *Optical Engineering*, Vol. 36, No. 1, 1997, pp. 56–72.
- Miller, E. R. (ed.), "STS-2,-3,-4 Induced Environmental Contamination Monitor (IECM) Summary Report," Marshall Space Flight Center, NASA TM-82524, Feb. 1983.
- Green, B. D., Rawlins, W. T., Caledonia, G. E., Marinelli, W. J., White, C., Simons, G. A., Gold, B., and Miranda, H., "The Determination of the Spacecraft Contamination Environment," U.S. Air Force Geophysics Lab. AFGL-TR-87-0303, Air Force Systems Command, Hanscom AFB, MA, Oct. 1987.
- Green, B. D., and Ahmadian, M., "The Variable Particle Environment Around the Shuttle," *Applied Optics*, Vol. 36, No. 6, 1977, pp. 1399–1406.
- Silver, D. M., "Midcourse Space Experiment Contamination Modeling," AIAA Paper 96-0223, Jan. 1996.
- Clifton, K. S., and Owens, J. K., "Optical Contamination Measurements on Early Shuttle Missions," *Applied Optics*, Vol. 27, No. 3, 1988, pp. 603–611.
- Cranmer, J. H., Sanders, J. T., Lesho, J. L., and Uy, O. M., "Contamination Control for the Midcourse Space Experiment, An Overview," *JHU/APL Technical Digest*, Vol. 17, No. 1, 1996, pp. 88–101.
- Mill, J. D., O'Neil, R. R., Price, S., Romick, G. J., Uy, O. M., Gaposchkin, E. M., Light, G. C., Moore, W. W., Murdock, T. L., and Stair, A. T., Jr., "The Midcourse Space Experiment: An Introduction to the Spacecraft, Instruments, and Scientific Objectives," *Journal of Spacecraft and Rockets*, Vol. 31, No. 5, 1994, pp. 900–907.
- Uy, O. M., Benson, R. C., Erlandson, R. E., Boies, M. T., Lesho, J. C., Galica, G. E., Green, B. D., Wood, B. E., and Hall, D. F., "Contamination Experiments in the Midcourse Space Experiment," *Journal of Spacecraft and Rockets*, Vol. 34, No. 2, 1997, pp. 218–225.
- Silver, D. M., Benson, R. C., Boies, M. T., Dyer, J. S., Erlandson, R. E., Galica, G. E., Green, B. D., Hall, D. F., Lesho, J. C., Phillips, T. E., Uy, O. M., and Wood, B. E., "Midcourse Space Experiment Molecular Contamination Modeling Predictions for Early Orbital Operations," *19th Space Simulation Conference, Cost Effective Testing for the 21st Century*, NASA Conf. Publication 3341, Oct. 1996, pp. 67, 68.
- Galica, G. E., Green, B. D., Atkinson, J. J., Aurillo, G., Shepherd, O., Lesho, J. C., and Uy, O. M., "Flashlamp Measurement of the MSX Particulate Environment," *Optical System Contamination: Effects, Measurements and Control V*, Vol. 2864, Proceedings of the Society of Photo-Optical Instrumentation Engineers, Denver, CO, 1996, pp. 169–180.
- Green, B. D., and Mulhall, P. A., "Particle Detection by Optical Systems on MSX," *Optical System Contamination: Effects, Measurement, and Control IV*, Vol. 2261, Proceedings of the Society of Photo-Optical Instrumentation Engineers, San Diego, CA, 1994, pp. 230–238.
- Israelachvili, J., *Intermolecular and Surface Forces*, Academic, London, 1992, Chap. 7.
- Green, B. D., Galica, G. E., Mulhall, P. A., Uy, O. M., Lesho, J. C., Boies, M. T., Benson, R. C., Phillips, T. E., Silver, D. M., Erlandson, R. E., Wood, B. E., Hall, D. F., and Mill, J. D., "Local Environment Surrounding the Midcourse Space Experiment Satellite in Its First Week," *Journal of Spacecraft and Rockets*, Vol. 35, No. 2, 1998, pp. 183–190.

R. G. Wilmoth  
Associate Editor